Electronic Supplementary Information

Nanostructured molybdenum phosphide/N, P dual-doped carbon nanotube composite as electrocatalysts for hydrogen evolution

Yang Zhao [a,c], Shuo Wang[a], Chunyan Li [a], Xianbo Yu [a], Chunling Zhu [b], Xitian Zhang, [c] Yujin Chen*[a,]

[a]*Key Laboratory of In-Fiber Integrated Optics, Ministry of Education, and College of Science,Harbin Engineering University, Harbin 150001, China. Fax: 86-451-82519754; Tel: 86-451-82519754; E-mail: chenyujin@hrbeu.edu.cn*

[b]*College of Materials Science and Chemical Engineering, Harbin Engineering University, Harbin, 150001, China. E-mail: chunlingzhu@hrbeu.edu.cn*

[c]*Key Laboratory for Photonic and Electronic Bandgap Materials, Ministry of Education, and School of Physics and Electronic Engineering, Harbin Normal University, Harbin 150025, China.*

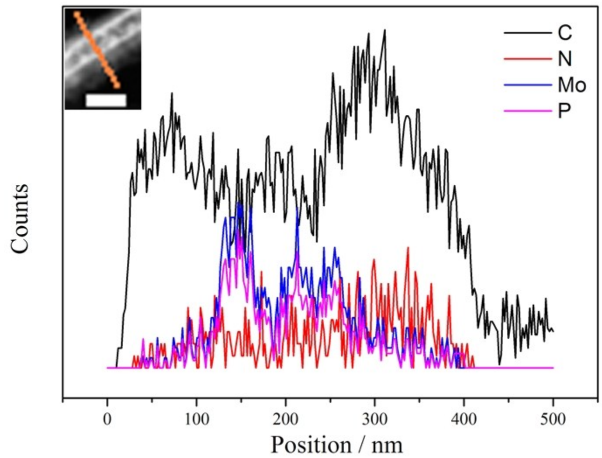

Figure S1. ADF STEM image and the corresponding EDX elemental scanning mappings of MoP/N,P–CNTs.

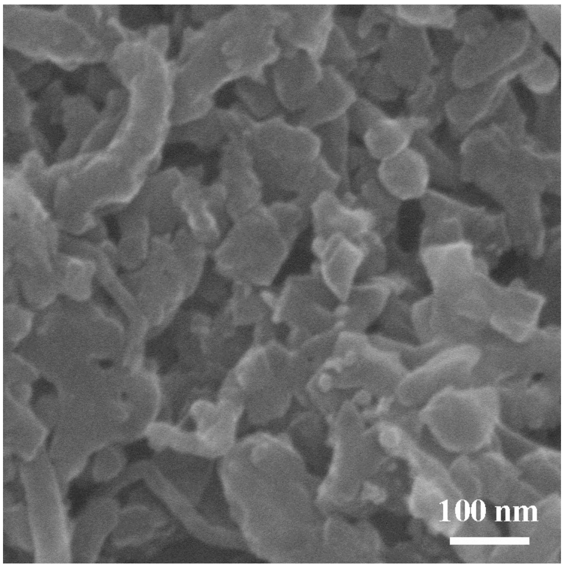

Figure S2. SEM image of P-PANI.

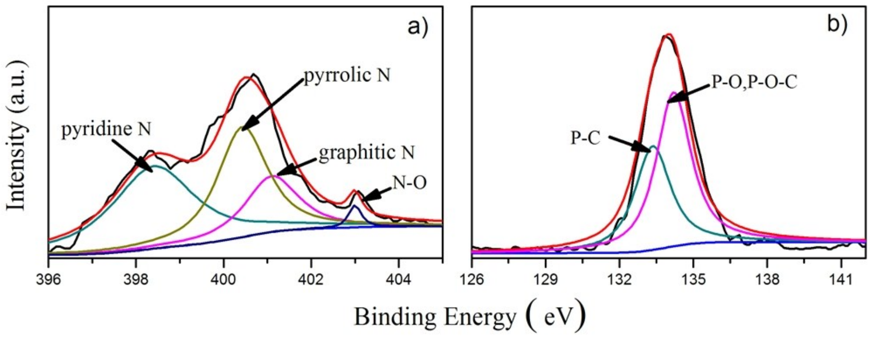

Figure S3 XPS spectra of P-PANI.

Table S1. The content of various elements in MoP/N,P–CNTs

MoP/N,P-CNTs at. %	C	N	O	P	Mo
XPS data	46.97	3.02	35.88	10.41	3.72
EDX data	58.87	3.85	23.06	10.77	3.45

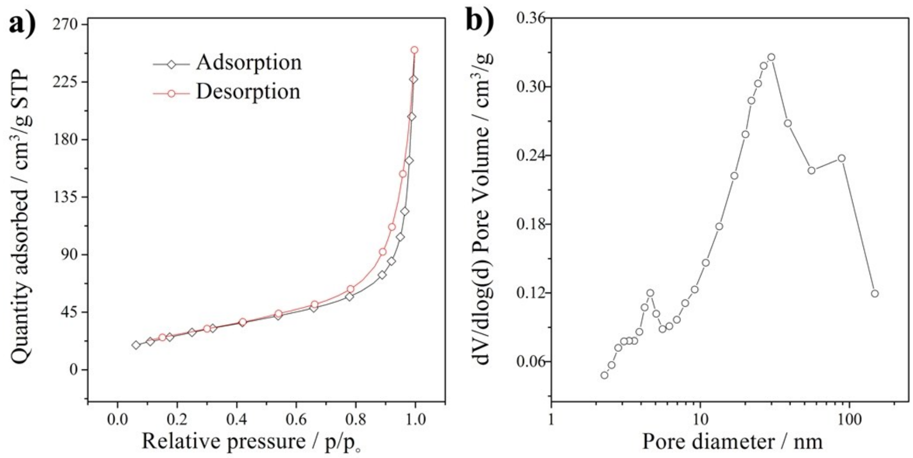

Figure S4. a) Nitrogen adsorption and desorption isotherms and b) the pore size distribution curve of MoP/N,P–CNTs.

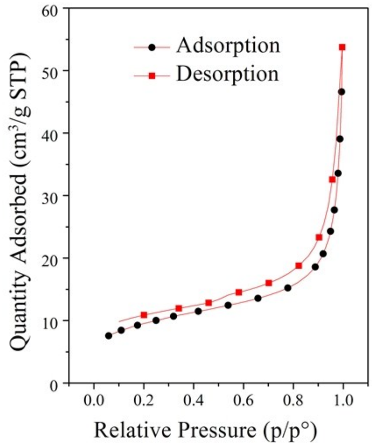

Figure S5. Nitrogen adsorption and desorption isotherms of MoO_2/N,P–CNTs.

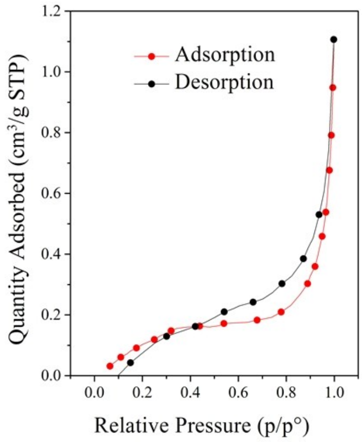

Figure S6. Nitrogen adsorption and desorption isotherms of bulk MoP.

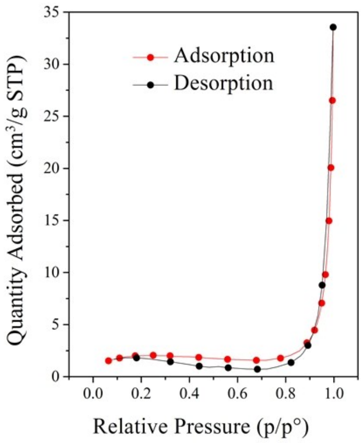

Figure S7. Nitrogen adsorption and desorption isotherms of P-PANI.

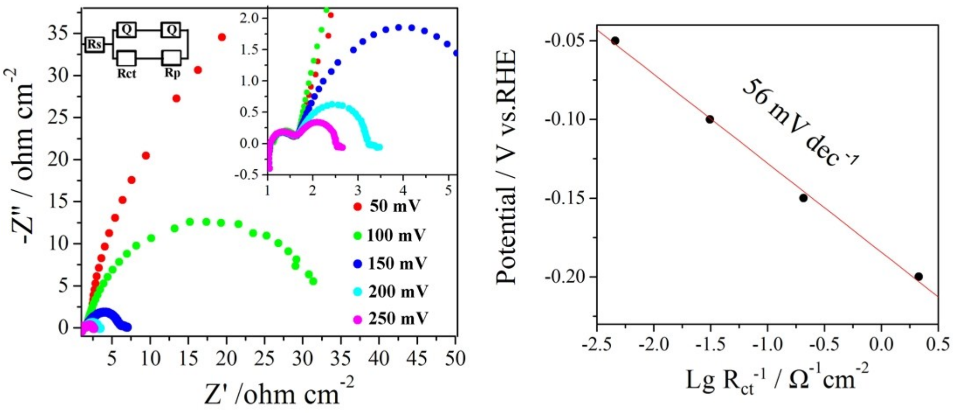

a) b)

Figure S8. a) Nyquist plots and the equivalent circuit and b) The plots of overpotential vs. lg R_{ct}^{-1} for MoP/N,P–CNT and its linear fitting for data obtained in 0.5 M H_2SO_4.

Table S2. Comparison of HER performance in acidic media of MoP/N,P–CNTs with other HER electrocatalysts

Catalysts	Tafel slope (mV dec^{-1})	j_0 (μA cm^{-2})	η_1 (mV)	η_5 (mV)	η_{10} (mV)	J_{200} (mA cm^{-2})	Refs.
FeP nanosheets	67	—	—	180	~240	6	3
MoP	60	4.15	~145	~200	246	~5	10
MoP-CA2	54	86	—	~105	125	100	13
MoP nanosheets	56.4	—	~100	~176	200	10	14
oxygen-incorporated MoS_2	55	12.6	—	~148	~170	19	17
MoS_2/Mo_2C-NCNTs	69	21	145	—	~190	15	19
Bulk MoS_2	120	—	87	—	260	3	19
MoS_2 nanoflowers	113	—	76	—	195	17	19
MoS_2 nanosheets	43	—	—	~175	`195	~25	21
Mo_2C/CNTGR	58	62	~62	~116	130	—	23
Mo_2N/CNTGR	72	39.4	~118	—	186	~15	23
Mo_2C/CNT	63	—	~120	—	190	~13	23
Cu_3P NW/CF	67	180	79	—	—	—	41

MoN/C	54.5	36	250	—	—	0.7	42
$NiMoN_x/C$	35.9	240	~148	—	—	3.5	42
Mo_2C/GCSs	62.6	12.5	~120	—	200	10	43
MoB	55	1.4	—	195	~211	~5.4	44
Mo_2C	56	1.3	~150	190	~208	~6.5	44
double-gyroid MoS_2/FTO	50	0.69	>150	~205	~230	~4.5	45
Co@NC/NG	79.3	—	—	150	~190	~14	46
FeS_2	56.4	0.144	217	—	N/A	1	47
CoS_2	52.0	3.53	128	173	192	—	47
NiS_2	48.8	0.0191	230	—	N/A	1	47
MoP/N, P-CNTs	**51**	**60**	**63**	**100**	**116**	**360**	**This work**

Note: η_1, η_5 and η_{10} denote overpotentials driving current densities of 1, 5 and 10 mA cm^{-2}, respectively. J_{200} denote the current density at an overpotential of 200 mV.

Table S3. Comparison of HER performance in alkaline media of MoP/N,P–CNTs with other HER electrocatalysts.

Catalysts	Tafel slope (mV dec^{-1})	j_0 (μA cm^{-2})	η_1 (mV)	η_{10} (mV)	J_{200} (mA cm^{-2})	Refs.
CoP/CC[a]	129	—	115	209	~24	9
MoP clusters	48	46	—	~132.5	—	12
MoB	59	2.0	~158	~216	~5.8	44
Mo_2C	54	3.8	~105	~171	—	44
MoP/N, P-CNTs	**58**	**100**	**62**	**117**	**135**	**This work**

Note: η_1 ,η_{10} and η_{10} denote overpotentials driving current densities of 1, 5 and 10 mA cm^{-2}, respectively. J_{200} denote the current density at an overpotential of 200 mV.

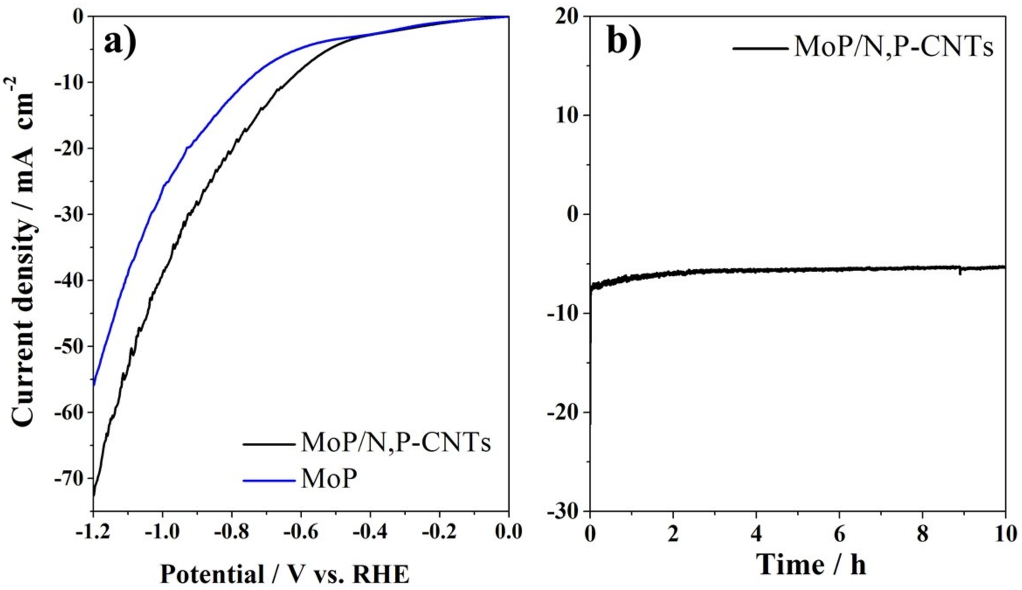

Figure S9. a) Polarization curves of MoP/N,P–CNTs in phosphate buffer and b) stability of MoP/N,P–CNTs at a given overpotential of 600 mV in phosphate buffer.

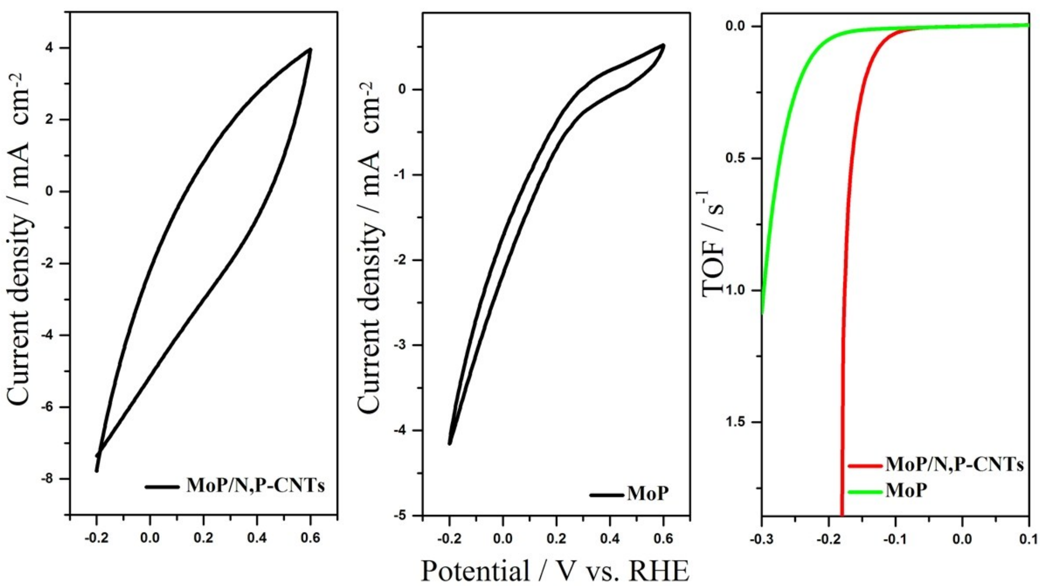

Figure S10. Cyclic voltammograms for MoP/N,P–CNTs a) and for b) bulk MoP in phosphate buffer, and c) TOF versus overpotential curves of MoP/N,P–CNTs and bulk MoP in 0.5 M H_2SO_4.

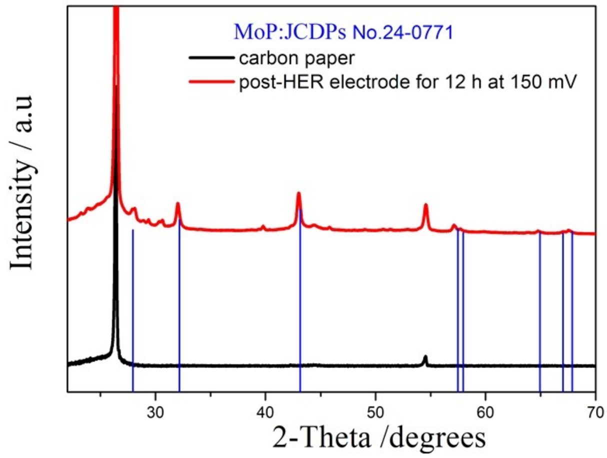

Figure S11. XRD pattern of the post-HER electrode after continuous water electrolysis at given overpotential of 150 mV for 12 h in 0.5 M H_2SO_4.

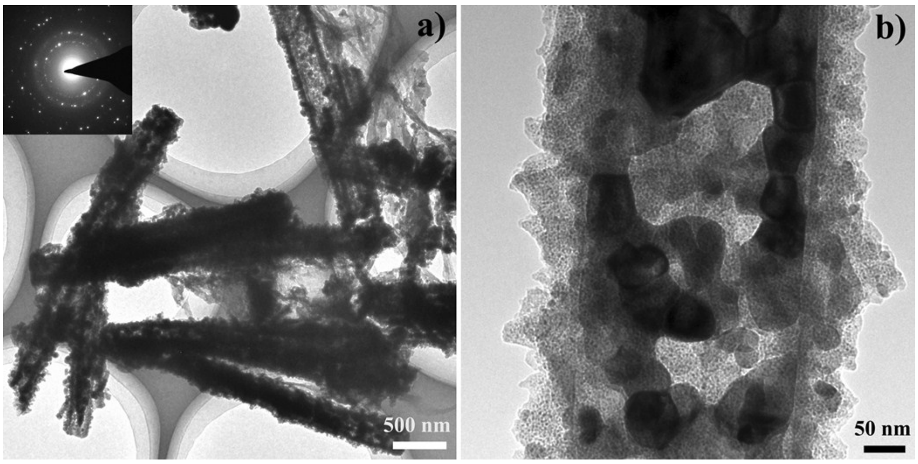

Figure S12. TEM images of MoP/N,P–CNTs scraped off from the post-HER electrode. a) Low-resolution TEM image and b) high-resolution TEM image, and the inset in a) shows the corresponding SAED pattern.

Table S4. Comparison the double layer capacitance (C_{dl}) in acidic media of MoP/N,P–CNTs with other HER electrocatalysts

Catalysts	C_{dl}(mF cm^{-2})	**Refs.**
P-WN/rGO	32	34

WN/rGO	11	34
Cu_3P NW/CF	77.8	41
Cu_3P MP/CF	4.1	41
Co@NC/NG	37.3	46
FeS_2	3.59	47
CoS_2	3.62	47
NiS_2	1.20	47
atomically-thin MoN nanosheets	1.56	49
bulk MoN	0.53	49
MoP/N, P-CNTs	**91**	**This work**

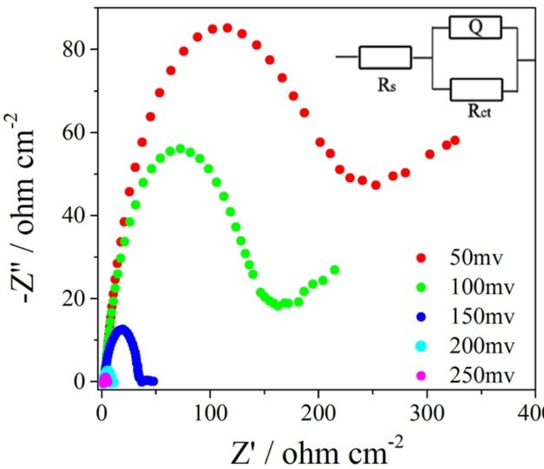

Figure S13. Nyquist plots and the equivalent circuit of the bulk MoP at various HER overpotentials in 0.5 M H_2SO_4.

Table S5. Comparison of charge-transfer resistances between bulk MoP and

MoP/N,P-CNTs at different overpotentials

R_{ct} (Ω cm^{-2}) \ η_i(mV)	100	150	200	250
Bulk MoP	175.5	36.7	7.3	3.2
MoP/N,P-CNTs	32.1	4.8	0.5	0.4

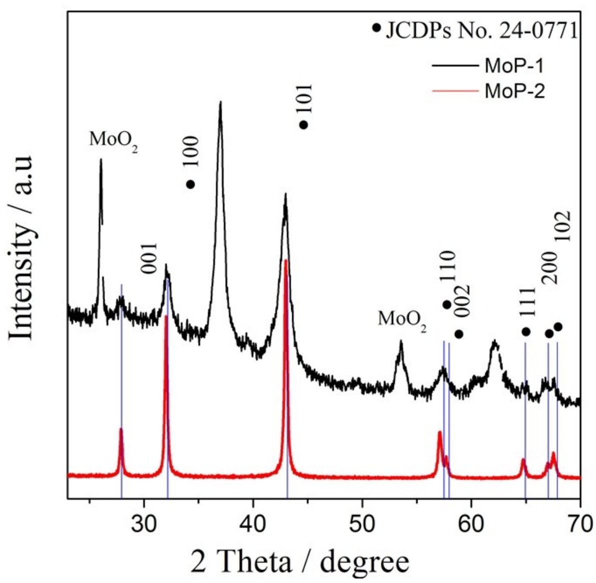

Figure S14. XRD patterns of MoP-1 and MoP-2.

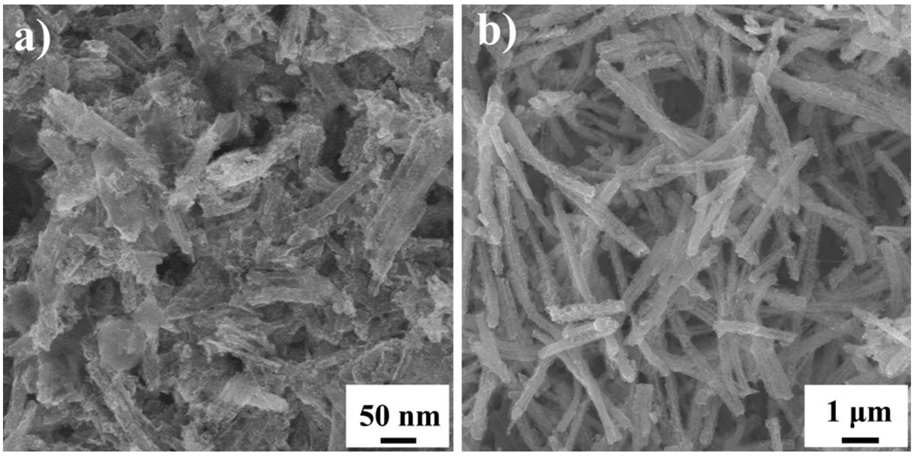

Figure S15. SEM images of MoP-1 (a) and MoP-2 (b).

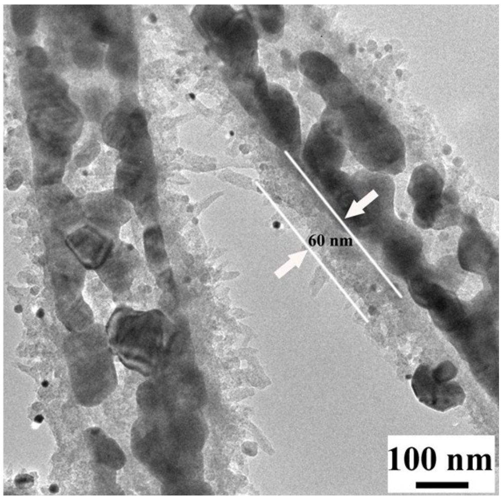

Figure S16. TEM image of MoP-2.

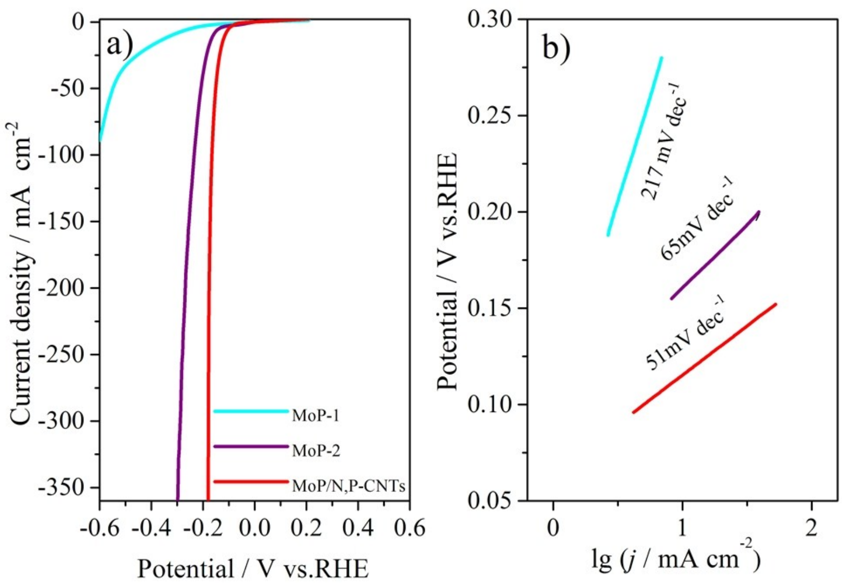

Figure S17. a) Polarization curves and b) Tafel plots of MoP/N,P–CNTs, MoP-1 and MoP-2 in 0.5 M H_2SO_4 solution.

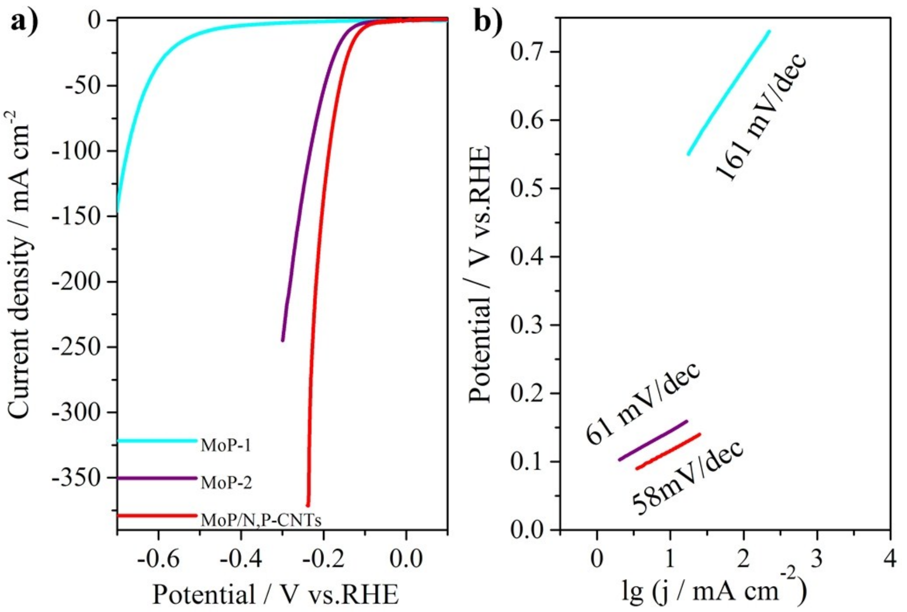

Figure S18 a) Polarization curves and b) Tafel plots of MoP/N,P–CNTs, MoP-1 and MoP-2 in 1.0 M KOH solution.

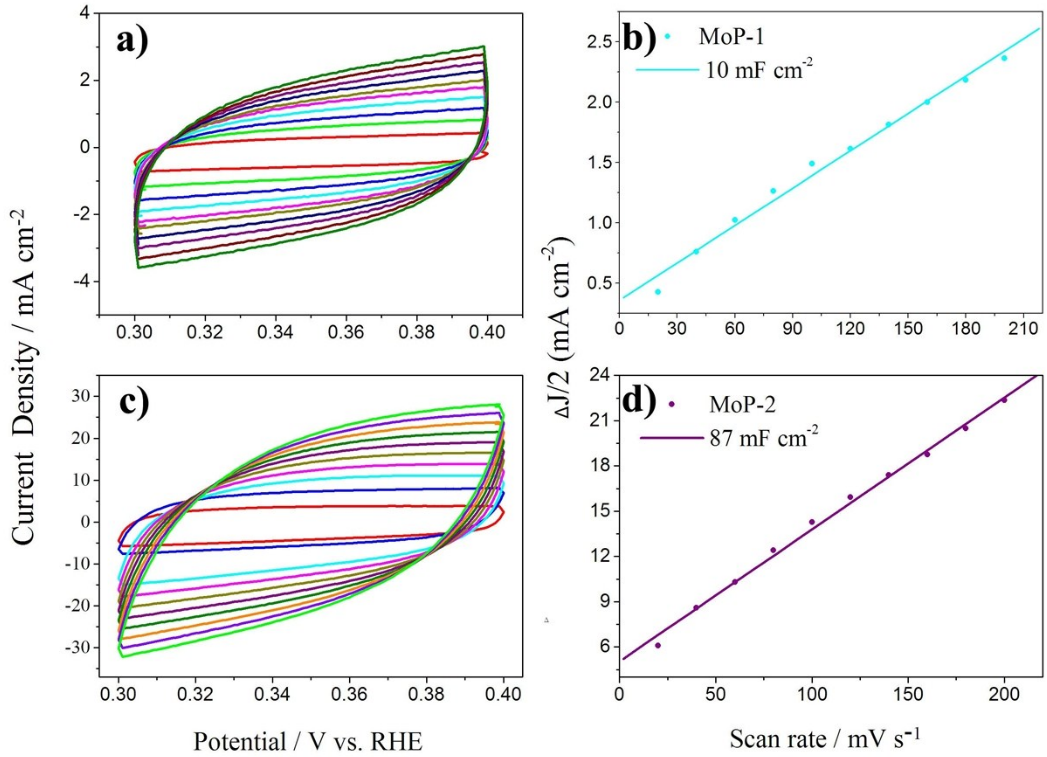

Figure S19 Cyclic voltammograms for (a) MoP-1 and (c) MoP-2 in the region of 0.3–0.4 V vs. RHE in 0.5M H_2SO_4; The differences in current density ($\Delta J = J_a\text{-}J_c$) for (b) MoP-1 and (d) MoP-2 at 0.35 V vs. RHE plotted against scan rate fitted to a linear regression allows for the estimation of C_{dl}.